

# High Efficiency Bus Provider for VLC Applications Based an Asymmetrical Half Bridge Converter with a Resonant DCX Auxiliary Output

Theyllor H. Oliveira, Manuel Arias, Diego G. Lamar, Daniel G. Aller, Abraham López.  
*Electrical, Electronic, Computers and Systems Engineering Department*  
 University of Oviedo.  
 Gijón, Spain.

hentschketheyllor@uniovi.es, ariasmanuel@uniovi.es, gonzalezdiego@uniovi.es, garciaadaniel@uniovi.es, lopezabraham@uniovi.es.

**Abstract**— The Two-Input Buck (TI Buck) Converter has low voltage stress over the switches, very high efficiency, and low harmonic components. Therefore, it is a prominent topology to work as a post-regulator in Visible Light Communication (VLC) systems. This works proposes a combination of an Asymmetrical Half Bridge (AHB) and a resonant dc-dc unregulated converter (DCX) to supply the two input voltage sources of the TI Buck based post-regulator. Due to the similarity in the primary side of these two converters (i.e AHB and DCX), the auxiliar DCX subcircuit will be coupled to the AHB without increasing the number of controlled switches. The topology, as well as the design constraints are studied in this paper. As example, a 45W AHB with an auxiliar DCX source is build. The topology reaches 94% of efficiency with the proposed independent behavior between the output voltages.

**Keywords** — *Asymmetrical Half Bridge, DCX, Two Input Buck, Resonant Circuit, Visible Light Communication, VLC.*

## I. INTRODUCTION

Light-emitting diodes (LED) are remarkable devices in light systems due to their high reliability, increasing light emission efficacy and chromatic variety. Also, its capacity of fast response to high frequency stimulus enables this technology to new applications as Visible Light Communication (VLC) [1][2]. Many ac-dc and dc-dc drivers have been proposed in literature to supply LED strings, and they can be classified according to the number of stages. One stage topologies are used for small size, low-cost solutions. Nevertheless, the Power Factor Correction (PFC) requirement normally leads to a high output current ripple or to the use of electrolytic capacitors, compromising lifespan and reliability. The two stage solutions normally use the first stage for PFC and the second stage for power regulation, including cancelling the output low frequency ripple. In specific applications like VLC, three stage drivers become interesting (Fig. 1) given the complex additional tasks to be carried out, separating the functions of PFC, voltage level regulation and modulation for communication purpose in three optimized stages.

The VLC drivers have two main functions, the regular ambient illumination, that can be achieved by fixing the average LED current, and the light intensity regulation for communication, through a given modulations scheme.

A prominent option for a post-regulator in a three stage dc-dc VLC driver is the Two-Input Buck (TI Buck) converter [3][4]. It presents a reduction in the switching losses, smaller passive elements and duty cycle resolution optimization. As a drawback of the TI Buck, two input voltage sources are needed. As will be explained in the section II, to meet the LED load characteristics (Fig. 2) one of the TI Buck input voltages should be a controllable source while the second

input voltage could be a fixed one. This normally implies the use of two independent converters, as each voltage have different requirements, or cross-regulated outputs of the same converter. Nevertheless, given the output voltages requirements, as fixed value, cross-regulated converters are not a valid option.

With the objective of optimizing a VLC driver using the TI Buch converter, this work proposes the development of an intermediate stage that efficiently meets the post-regulator necessities.

The first voltage will be supplied by the Asymmetrical Half Bridge (AHB) converter, being a controlled high efficiency topology [5][6].The second voltage source, which is fixed, will be obtained by an auxiliary circuit based on a resonant topology based on a dc-dc unregulated converter (DCX) [7][8]. The main advantage of the DCX is that its output voltage is constant and independent from the duty cycle. In this way, both, the AHB and the DCX, can share the input half bridge, achieving two independent outputs without increase the number of transformers and MOSFETs.

The paper is organized as follows. For the sake of clarity, section II provides a brief description of the involved topologies, which will serve as introduction for the proposed idea. The TI Buck will be defined in section II-A, the circuit basic operation of the AHB topology will be presented in the section II-B and in section II-C a brief review of the resonant DCX will be carried out. The entire combination concept will be developed in section III, as well as the consequent boundaries arising from this proposal with a recommended design workflow. To validate the topology, an analysis of a 45W prototype will be shown in the Section IV and the conclusions will be presented in the Section V.

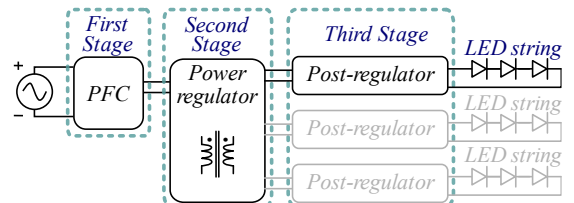


Fig. 1. VLC system concept.

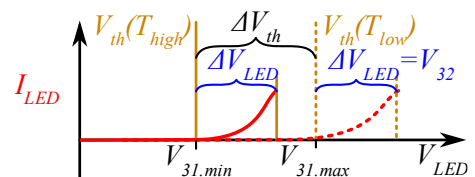


Fig. 2. IV LED curve behavior for temperature variations from high values ( $T_{high}$ ) to low values ( $T_{low}$ ).

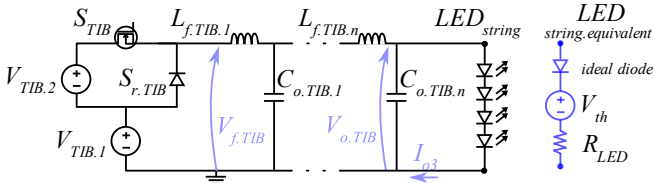


Fig. 3. TI Buck configuration and LED string equivalent circuit.

## II. PRELIMINAR DESCRIPTION OF THE INVOLVED TOPOLOGES

### A. TI Buck Definition

The Fig. 3 presents the TI Buck topology. It presents a similar static gain of a traditional buck converter plus an offset supplied by the series source  $V_{TIB.1}$ :

$$V_{o.TIB} = V_{TIB.1} + V_{TIB.2} \cdot D_{TIB} \quad (1)$$

where  $D_{TIB}$  is the TI Buck duty cycle.

The value of the input voltage  $V_{TIB.1}$  will be defined by the LED operational temperature, since a higher temperature results in a threshold voltage ( $V_{th}$ ) reduction caused by the LED thermal coefficient. On the other hand,  $\Delta V_{LED}$  is independent from temperature, making  $V_{TIB.2}$  independent from this parameter. As can be seen, the topology perfectly suits the LED electrical behavior (Fig. 2). The threshold voltage ( $V_{th}$ ) is supplied by  $V_{TIB.1}$ , while  $V_{TIB.2}$ , along with  $D_{TIB}$ , allows to perfectly control the LED luminance, and therefore performing the lighting and communication tasks among the overall reduction of the IV curve [4].

### B. AHB as the base Isolated Second Stage

The AHB topology is shown in Fig. 4. The two switches work with complementary signals, and the duty cycle in this converter is always lower than 50% [5].

As a consequence of the voltage-second balance in the transformer, the duty cycle ( $D_{AHB}$ ) variation changes the steady-state voltage in  $C_1$  and  $C_2$ :

$$V_{C1} = (1 - D_{AHB}) \cdot V_g, \quad (2)$$

$$V_{C2} = D_{AHB} \cdot V_g, \quad (3)$$

where,  $V_g$  is the input voltage,  $V_{C1}$  and  $V_{C2}$  are the voltages in the capacitors  $C_1$  and  $C_2$  respectively.

The switching process applies  $V_{C1}$  and  $V_{C2}$  voltages to the transformer. The reflected voltages in the secondary are applied to the output filter by the action of rectifiers. The resulting waveform is easier to be filtered, reducing the filter volume [5]. The voltage-second balance in the output inductor ( $L_{fl}$ ) leads to the output voltage ( $V_{o.AHB}$ ):

$$V_{o.AHB} = V_{C1} \cdot D_{AHB} \cdot \frac{N_1}{N_p} + V_{C2} \cdot (1 - D_{AHB}) \cdot \frac{N_2}{N_p}, \quad (4)$$

where,  $N_p$ ,  $N_1$  and  $N_2$  are the AHB primary and secondary turn ratio (see Fig. 4).

Assuming that the input voltage is provided by a PFC without electrolytic capacitor, the ripple cannot be neglected. Therefore, the maximum duty cycle ( $D_{max}$ ) must ensure the maximum output voltage ( $V_{o.AHB,max}$ ) with the minimum input voltage value ( $V_{g,min}$ ). Based on eq. (2)-(4) the conditions could be described by (5). The  $D_{max}$  value could be considered 50% of the switching period ( $T_s$ ) decreased ideally only by the dead time ( $t_d$ ) between the gate signals.

$$V_{O1,max} = V_{g,min} \cdot D_{max} \cdot (1 - D_{max}) \cdot \left( \frac{N_1}{N_p} + \frac{N_2}{N_p} \right). \quad (5)$$

The  $t_d$  is necessary for the Zero Voltage Switching (ZVS) process. A detailed analysis of the ZVS is presented in [9],

where the total energy stored in the magnetizing inductance ( $L_m$ ) is studied as the way for exchange the energy in the MOSFET output capacitors ( $C_{oss}$ ).

Given the AHB particular control, the average value of the magnetizing current of the transformer is not necessary zero. Therefore, for an optimized AHB design a specific turn ratio should be set for each secondary winding to perform a reduction on the average magnetizing current, also reducing power losses.

$D_{Lm0}$  defines the operation where the average magnetizing current is zero [9]. First, a variation of Eq. (4) is used for  $D_{Lm0}$  with the nominal values of  $V_g$  and  $V_{o.AHB}$  obtaining (6). Then, the  $N_2$  definition (7) (detailed in [9]), could be associated with the previous equations to design  $N_2$  and  $N_1$ , and so, the AHB transformer. Following Eq. (5), the same development could be applied to define  $D_{min}$  for the minimal  $V_{o.AHB}$  ( $V_{o.AHB,min}$ ) and maximal  $V_g$  value ( $V_{g,max}$ ):

$$V_{o.AHB} = V_g \cdot D_{Lm0} \cdot (1 - D_{Lm0}) \cdot (N_1 + N_2), \quad (6)$$

$$N_2 = N_1 \cdot \frac{D_{Lm,0}}{1 - D_{Lm,0}}, \quad (7)$$

$$V_{o.AHB,min} = V_{g,max} \cdot D_{min} \cdot (1 - D_{min}) \cdot (N_1 + N_2). \quad (8)$$

### C. Resonant DCX

Fig. 5 shows the resonant DCX on which the proposed auxiliary circuit is based. The leakage inductance ( $L_k$ ) and the output capacitor ( $C_r$ ) define the resonant tank. This leads to a very simple topology with high efficiency as ZVS and ZCS can be achieved [7]. The main drawback is a high-frequency ripple in the output voltage, which can be easily attenuated by a small-size filter.

In the DCX, the duty cycle is fixed on 50%. This leads to an output voltage ( $V_{o.DCX}$ ) defined by:

$$V_{o.DCX} = V_g \cdot \frac{N_s}{2}. \quad (9)$$

## III. DCX AS AUXILIARY SECOND STAGE DESIGN

The AHB and the DCX present a similar half-bridge and transformer at their inputs, with the only difference being the lack of the  $L_{f.AHB}$  in the DCX secondary (see Fig. 4 and Fig. 5). Due to the primary side similarity, is possible to combine both topologies to achieve two outputs without increase the number of MOSFETs and transformers.

The AHB structure still unchanged. As a result,  $V_{o.AHB}$  can be controlled through duty cycle ( $D_{AHB}$ ). The inclusion of the DCX-derived auxiliary circuit needs a more detailed description. First, each secondary winding connects, by the diode, to its own output capacitor. This culminates in two independent resonant circuits.

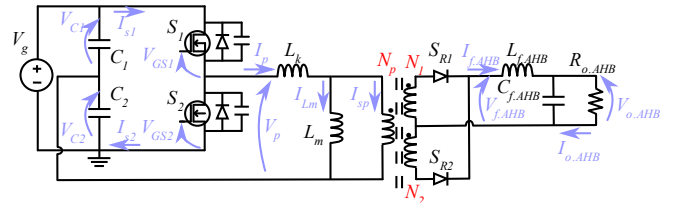


Fig. 4. AHB topology.

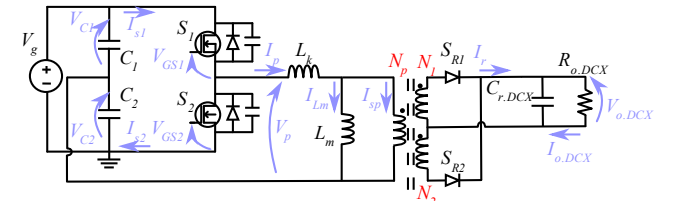


Fig. 5. Resonant DCX topology.

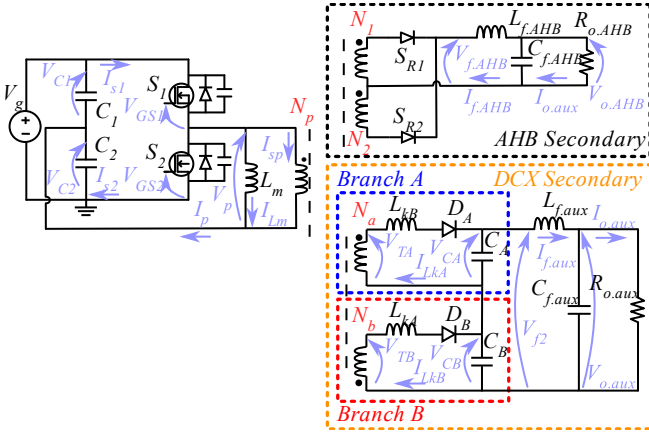


Fig. 6. Proposed AHB with auxiliary resonant DCX topology.

Applying the volt-second balance to each leakage inductance results in:

$$V_{CA} = \frac{N_a}{N_p} \cdot V_{C1}, \quad (10)$$

$$V_{CB} = \frac{N_b}{N_p} \cdot V_{C2}. \quad (11)$$

Given  $C_A$  and  $C_B$  serial connection, the output voltage ( $V_{o,aux}$ ) is defined as:

$$V_{o,aux} = V_{CA} + V_{CB} = \frac{N_a}{N_p} \cdot V_{C1} + \frac{N_b}{N_p} \cdot V_{C2}, \quad (12)$$

replacing  $V_{C1}$  and  $V_{C2}$  by the values in equations (2) and (3), the output voltage is defined by:

$$V_{o,aux} = \frac{N_a}{N_p} \cdot (1 - D_{AHB}) \cdot V_g + \frac{N_b}{N_p} \cdot D_{AHB} \cdot V_g, \quad (13)$$

and assuming  $N_a$  equal to  $N_b$ :

$$V_{o,aux} = \frac{N_a}{N_p} \cdot V_g. \quad (14)$$

Equation (14) shows that the voltage provided by this auxiliary output is constant and independent of  $D_{AHB}$ , which is used to regulate  $V_{o,AHB}$ . In this way, both voltages adapt perfectly to the needs of the TI Buck in order to be used as a post-regulator for a three-stage ac-dc VLC driver.

The mains waveforms for a soft switching configuration are presented in Fig. 7. As the two secondaries subcircuits work almost independently, the topology will present many different operational stages. For a better comprehension, the operational stages will be explained in section A, and the analysis of the design will be presented in section B.

#### A. Operational Stages Description

##### 1) First Stage, $t_0$ to $t_1$ :

The switching process starts when the  $V_{GS1}$  turns on. The voltage  $V_{C1}$  is applied to the transformer primary side, and reflected to the secondary windings, as illustrated by the equivalent circuit shown in Fig. 8.

The AHB filter inductor current ( $I_{f,AHB}$ ) has a positive slope because the reflected  $V_{C1}$  value is bigger than  $V_{o,AHB}$ . In the DCX secondary side, the voltage  $V_{TA}$  is speedily bigger than  $V_{CA}$  and, as a result, the resonance between  $L_{kA}$  and  $C_A$  was already started (see the fourth stage, Fig. 11, section III.A.4). The filter inductor  $L_{f,aux}$  also maintains a positive and permanent current flow, discharging both output capacitors.

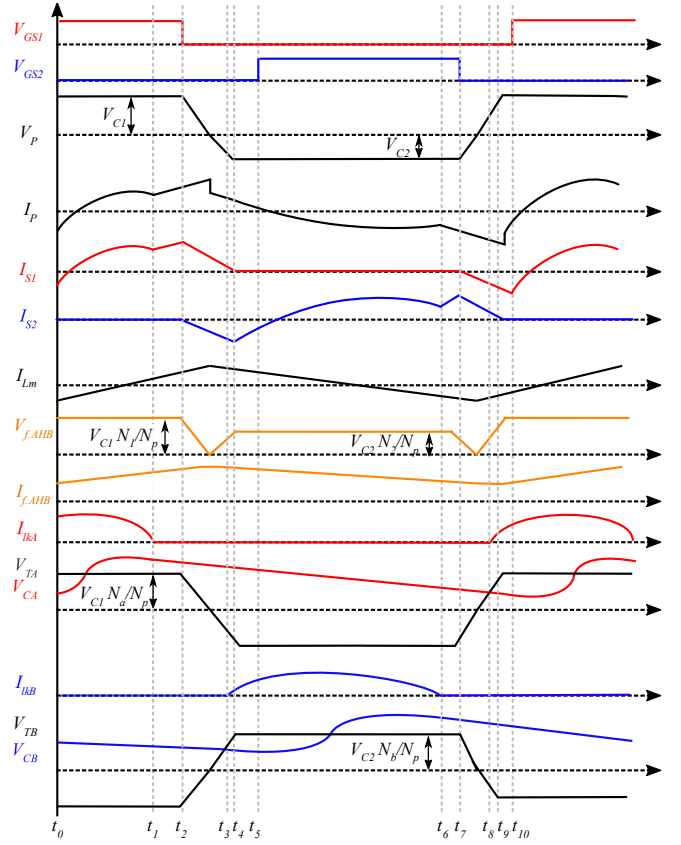


Fig. 7. Simplified waveforms for an AHB with a resonant DCX auxiliary output.

##### 2) Second stage, from $t_1$ to $t_2$ :

In the second stage the diode  $D_A$  blocks the resonant current flow in the negative direction. Thus, the resonant capacitors are only discharged by the current  $I_{f,aux}$ . For the AHB, the second operational stage is similar to the first stage.

The circuit presented in Fig. 9 is valid for this stage until the gate signal  $V_{GS1}$  changes, turning off the MOSFET  $S_1$ .

##### 3) Third stage, from $t_2$ to $t_3$ :

With the MOSFET  $S_1$  turn off, the circuit goes into the dead time interval, promoted by the two primary gate signals. With a proper design, the residual magnetizing current is forced to follow through the MOSFET's output capacitors, providing ZVS, as in a regular AHB converter.

Fig. 10 shows the equivalent circuit during the dead time. The components that will be part of the dead time state transitions are highlighted in orange. Initially, the current flows through diode  $S_{R1}$ . The primary voltage  $V_p$  equals the value of  $S_2$  output capacitor voltage ( $V_{Coss2}$ ) minus  $V_{C2}$  value. As  $V_{Coss2}$  discharges,  $V_p$  decreases and became negative, changing the voltage polarity in AHB secondary windings. Consequently, the diode  $S_{R1}$  will be reverse biased and the diode  $S_{R2}$  start to drive  $I_{f,AHB}$ .

The resonant DCX auxiliary output is stills working with the same behavior as the previous stage, until  $V_{TB}$  becomes bigger than the  $V_{CB}$  (due to  $V_p$  changes). This change turn on the diode  $D_B$  and start a second resonance, marking the beginning of the next stage.

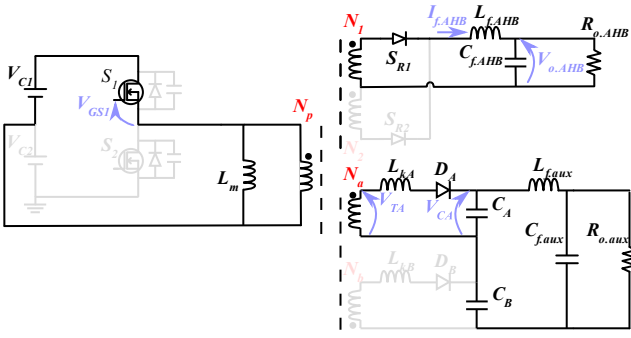


Fig. 8. Equivalent circuit of the first stage ( $t_0$  to  $t_1$ ).

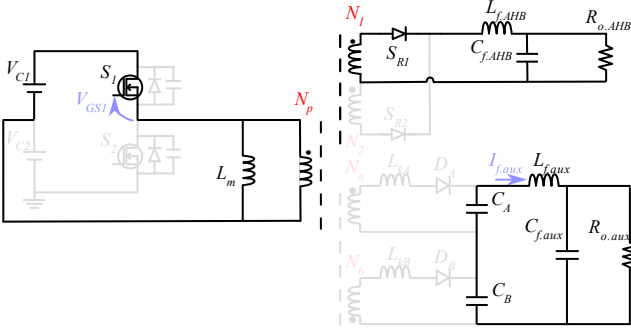


Fig. 9. Equivalent circuit of the second stage ( $t_1$  to  $t_2$ ).

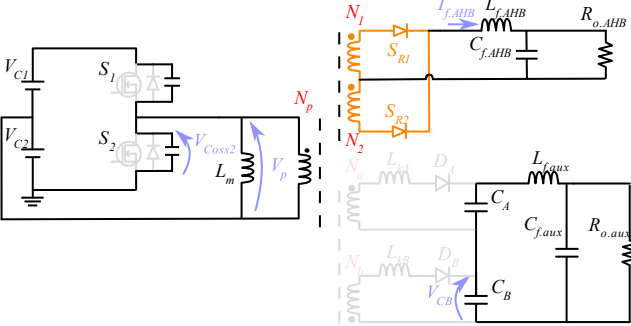


Fig. 10. Equivalent circuit of the third stage ( $t_2$  to  $t_3$ ).

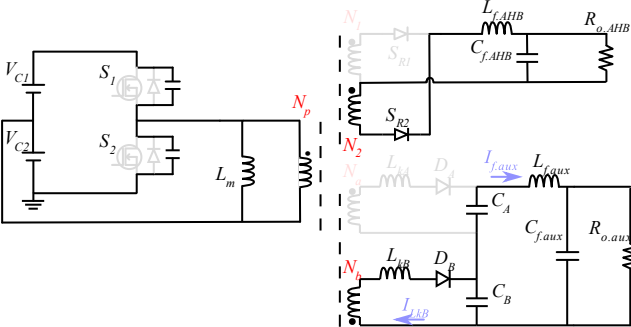


Fig. 11. Equivalent circuit of the fourth stage ( $t_3$  to  $t_4$ ).

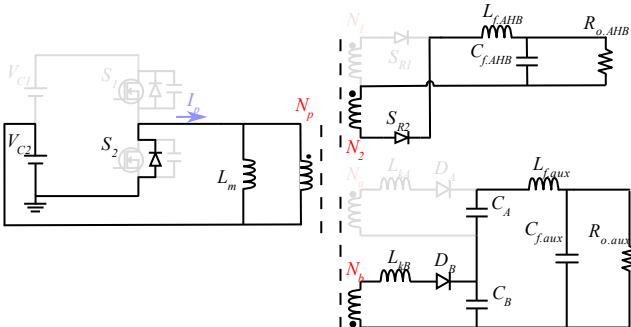


Fig. 12. Equivalent circuit of the fifth stage ( $t_4$  to  $t_5$ ).

#### 4) Fourth stage, from $t_3$ to $t_4$ :

The fourth stage is marked by the start of the resonance in the branch B of the resonant DCX auxiliary output. The  $I_{Lk,b}$  current starts to charge  $C_B$  while the current  $I_{f,aux}$  still discharging both output capacitors, defining the equivalent circuit presented in Fig. 11. This process will last until the capacitor  $C_{oss2}$  complete discharges and the  $S_2$  diode starts to drive current, clamping the voltage of the transformer primary side to the  $V_{C2}$  value.

#### 5) Fifth stage, from $t_4$ to $t_5$ :

In the fifth stage, both secondary outputs work with the same behavior as the last stage, as represented in Fig. 12. While  $I_p$  still positive,  $S_2$  can switch in a ZVS condition. The change for next stage is marked by the  $S_2$  gate signal, that changes the current flow from the diode to the MOSFET main path, with no more impact in the equivalent circuit. The sixth stage starts a new cycle that mimics the behavior of the first five stages, therefore the rest of the analysis can be obviate.

### B. Resonant Tank Design

First, for the resonant DCX auxiliary output design, a generic LC circuit, as the one shown in Fig. 13, could be assumed following [8]. In the equivalent circuit,  $L_{lk,aux}$  represents  $L_{kA}$  or  $L_{kB}$ , and  $C_o$  represents  $C_A$  or  $C_B$ , defined by the branch that will be analyzed. The voltage of primary capacitors ( $V_{CP}$ ) are considered again as voltage sources and the resonant current ( $I_{lk}(t)$ ) initial value equals zero. Fig. 13 is valid for times from zero to the resonant time for  $I_{lk}(t)$  reaches zero ( $t_{res}$ ).

The equations for  $I_{lk}(t)$ , the capacitors voltage time function ( $V_{Co}(t)$ ), and the natural frequency ( $\omega_0$ ) for the equivalent circuit in figure Fig. 13 are defined in (15)-(17).

$$I_{lk}(t) = \left( \frac{n_{aux}}{n_p} V_{CP} - V_{Co}(0) \right) \cdot \sqrt{C_o \cdot L_{lk}^{-1}} \cdot \sin(\omega_0 t) + I_{o2} \cdot (1 - \cos(\omega_0 t)), \quad (15)$$

$$V_{Co}(t) = V_{Co}(0)(\cos(\omega_0 t)) + \frac{n_{aux}}{n_p} V_{CP}(1 - \cos(\omega_0 t)) - I_{o2} \sqrt{C_o \cdot L_{lk}^{-1}} \cdot \sin(\omega_0 t), \quad (16)$$

$$\omega_0 = (\sqrt{C_o \cdot L_{lk}})^{-1}. \quad (17)$$

During the remaining part of the period, the voltage in  $C_o$  discharges linearly with  $I_{f,aux}$ . Thus, the initial value of  $V_{Co}$  ( $V_{Co}(0)$ ) is defined by the  $V_{Co}$  voltage at  $t_{res}$  ( $V_{Co}(t_{res})$ ) decreased by the effect of  $I_{o,aux}$  (18).

$$V_{Co}(0) = V_{Co}(t_{res}) - I_{o,aux}(T_s - t_{res})(2C_o)^{-1}, \quad (18)$$

As shown in figure Fig. 7, for the optimal operation of the resonant DCX auxiliary output, the resonant currents in auxiliary branches ( $I_{LkA}$  and  $I_{LkB}$ ) must cease before the PWM signal changes the voltage polarity of the primary and secondary windings. If not, the ZVS would not be achieved, and the efficiency would be drop.

For a proper operation of the TI Buck converter acting as a post-regulator of the ac-dc three stage VLC driver, with the variation of the voltage  $V_{th}$ , the AHB circuit will perform a variation in the duty cycle that changes the period and the amplitude of the voltages in the secondary windings. Each branch (A and B) operates in complementary periods. Therefore, to avoid that  $t_{res}$  became longer than the available time, as shown in Fig. 14, individual limits must be set.

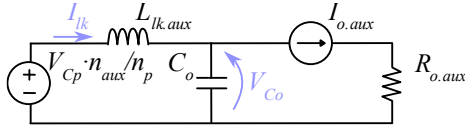


Fig. 13. Equivalent circuit of the resonant DCX auxiliary output branches (valid for time values between zero and  $t_{res}$ ).

The limit for  $t_{res}$  is directly proportional to the duty cycle for branch A and inversely proportional for branch B. As described in Section II.A.4, the resonant current can start during the dead time. However, the start's instant can change for different operating points and the limit should be restricted to the worst case (i.e. with the resonance starting at the end of the dead time). Given these considerations, the limits  $t_{a,min}$  and  $t_{b,min}$  for complete the overall resonance of the currents  $I_{LkA}$  and  $I_{LkB}$  are:

$$t_{a,min} = T_s \cdot D_{min} - t_d, \quad (19)$$

$$t_{b,min} = T_s \cdot (1 - D_{max}) - t_d, \quad (20)$$

For the resonant tank definition, first the AHB circuit must be designed. Based on the transformer values, the secondary windings of the resonant DCX auxiliary output can be defined and  $L_{kA}$  and  $L_{kB}$  values must be computed.

Based on Eq. (15)-(18), for a fixed  $L_{ik}$ , different  $t_{res}$  are obtained for different  $C_o$  values. Fig. 15 shows  $t_{res,A}$  (red line) and  $t_{res,B}$  (blue line) variation, for a given leakage inductances, as a function of  $C_o$ . The capacitance choosing must prioritize the highest commercial values that respect the limits imposed by  $t_{a,min}$  and  $t_{b,min}$  (dashed lines). Otherwise, small capacitances can generate higher current peaks with short periods, which increase the component losses and electromagnetic interferences.

To exemplify the entire design a 45W prototype of the AHB with an auxiliar DCX was made (Fig. 16), and the experimental results will be presented in the next section.

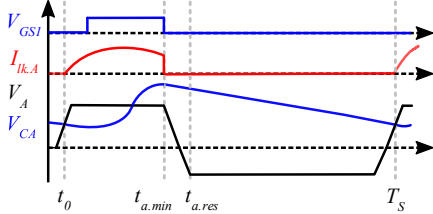


Fig. 14. Resonance cutting in DCX auxiliary output in Branch A.

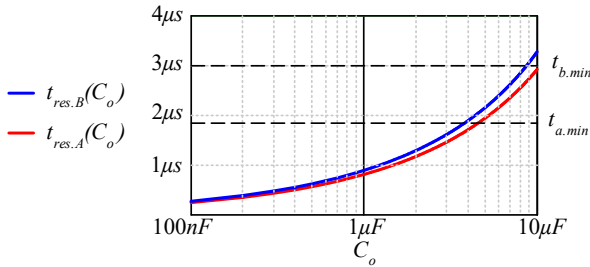


Fig. 15. Graphical design source.

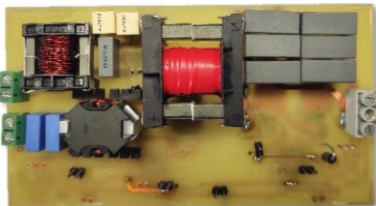


Fig. 16. AHB with resonant DCX auxiliary output prototype.

#### IV. EXPERIMENTAL RESULTS

A prototype of the AHB with the auxiliary resonant circuit has been built to validate the proposal (see Fig. 16). This circuit is designed to supply a LED string up to 45-W, with 41-W managed by the main converter (AHB) and 4-W supplied by the auxiliary circuit. The LED string is composed by 15 units of the *JR5050AWT-Q-B50EB0000* LED, that has a  $V_{th}$  of 5.5-V ( $\pm 200$ -mV) for 25- $^{\circ}$ C and a thermal coefficient of -2-mV/ $^{\circ}$ C. The LED operation was assumed for temperatures from 0 to 100- $^{\circ}$ C. Consequently, as represented in Fig. 2, the TI Buck post-regulator demands a  $V_{TIB.1,max}$  of 83-V to supply the LED  $V_{th}$  at the pick temperature and a  $V_{TIB.1,min}$  of 74.5-V to supply the  $V_{th}$  at the lower temperature. In addition, the TI Buck demands a voltage  $V_{TIB.2}$  of 16.5-V to supply the  $\Delta V_{LED}$ . The average LED current is 500-mA, and the average duty cycle for the post-regulator is 50%.

The AHB switching frequency is 120-kHz and the bridge MOSFETs are *STD13N65M2*. Three parallel 220-nF film capacitors compound  $C_1$  and  $C_2$  and two IPD60R360P7S are utilized for a synchronous rectification in the secondary. The  $D_{max}$  is defined as 50% with a  $t_d$  of 7%, what leads, with Eq. (2)-(8), for a  $D_{min}$  of 27%. Thus, with an input voltage of 400-V ( $\pm 7\%$ ), the normalized values for  $n_1$  and  $n_2$  are respectively 0.687 and 0.306. Finally, the transformer was designed with a magnetizing inductance of 465- $\mu$ H in a EE25 core with 42 primary turns.

According to Eq. (14), the DCX auxiliary windings were made with 2 turns, resulting in a  $L_{LkA}$  of 125-nH and a  $L_{LkB}$  of 139-nH. This leads to a 16,5-V / 200-mA output. Equations (15)-(17) along with the limits calculated with Eq. (19)-(20) defines a 2.2- $\mu$ F film capacitor for  $C_A$  and two parallel capacitors of 4.7- $\mu$ F for the  $C_B$ .

The output voltages  $V_{o,AHB}$  and  $V_{o,Aux}$  are shown in Fig. 17 for different duty cycle values.

In Fig. 18, the behavior of  $I_{LkA}$  current at  $D_{max}$  (a) and  $D_{min}$  (b) are shown. The resonant time is almost the same in these two conditions, just the peak value changes due to the input voltage variation. In addition, the  $I_{LkB}$  behavior presented in Fig. 19.(a) and (b) ( $D_{min}$  and  $D_{max}$ , respectively) works in a similar way. Fig. 19 shows the effect of parasitic resistances in the resonant current. Due to the excessive dumping effect, the current does not reach zero, loosing ZCS. Although its value is considerably small, and the associated losses are very low. A suitable design of the transformer, along with the correct component selection, could solve the problem, shown in Fig. 19.(b) for the same resonant circuit.

The Fig. 20 shows the circuit overall efficiency ( $\eta$ ) for different input voltages. The circuits present a limited efficiency variation changing the duty cycle from  $D_{min}$  to  $D_{max}$ .

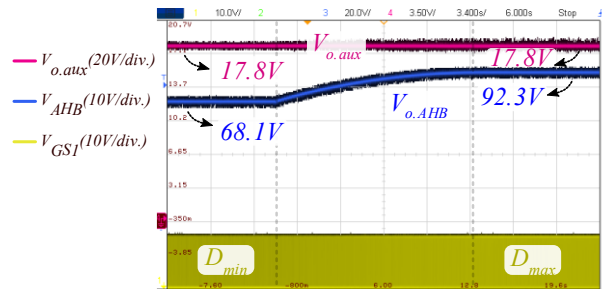


Fig. 17.  $V_{o,AHB}$  (blue) and  $V_{o,Aux}$  (magenta) behavior as function of the  $D_{AHB}$  variation from  $D_{min}$  to  $D_{max}$ , for  $V_g$  of 400V.

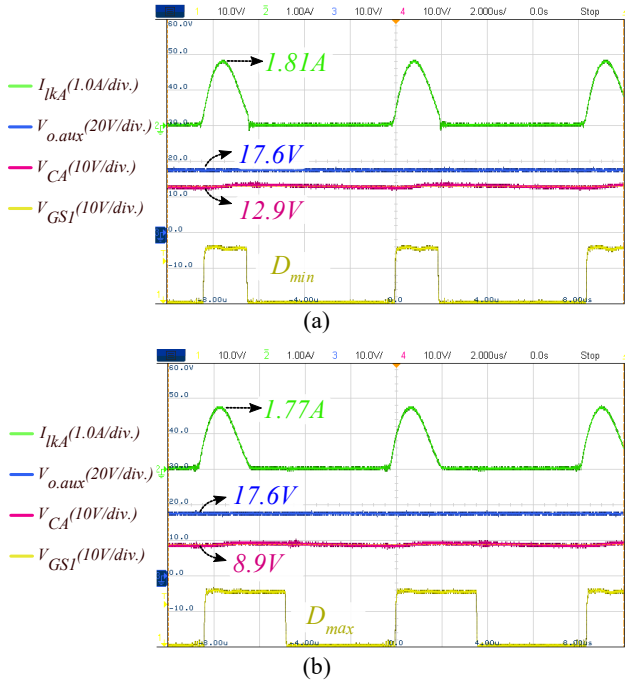


Fig. 18.  $I_{ikA}$  (green),  $V_{CA}$  (magenta) and  $V_{o.aux}$  (blue) behavior from DCX auxiliary output branch A for (a) $D_{max}$  and (b) $D_{min}$ .

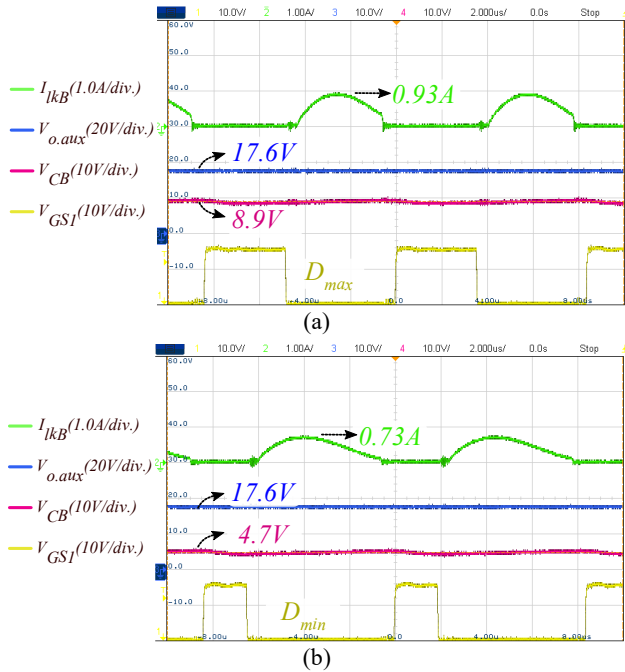


Fig. 19.  $I_{ikB}$  (green),  $V_{CB}$  (magenta) and  $V_{o.aux}$  (blue) behavior from DCX auxiliary output branch B for (a) $D_{max}$  and (b) $D_{min}$ .

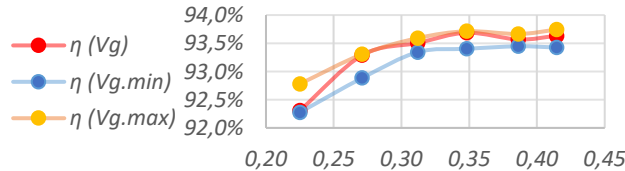


Fig. 20. Prototype efficiency as a function of the duty cycle.

## V. CONCLUSION

In this work, a AHB circuit with an auxiliary output based in resonant DCX was presented. This circuit is proposed as a second stage in a VLC system, for supplying a TI Buck as post-regulator.

The first and third stages was used to delimit the duty values and the input and output voltages. Then the AHB design defined the transformer and the leakage inductances from the DCX windings are used to find the resonant time and delimit the capacitor's choice.

The results obtained for a 45W prototype shows that the driver can supply two independent charges, maintaining the efficiency at different operating points with two independent output voltages. In addition, the results shows that  $V_{O.aux}$  is fixed for all duty cycle range. In contrast, the  $V_{O.AHB}$  changes from under the required  $V_{TIB.1.min}$  to over the required  $V_{TIB.1.max}$ , covering any operational value.

## VI. ACKNOWLEDGMENTS

This work has been carried out by funding from the Spanish government through the RTI2018-099682-A-I00 project, under the PRE2019-088425 grant, and by the Principality of Asturias under the scholarship BP17-91.

## REFERENCES

- [1] D. Karunatilaka, F. Zafar, V. Kalavally, and R. Parthiban, "LED based indoor visible light communications: State of the art," *IEEE Commun. Surv. Tutorials*, vol. 17, no. 3, pp. 1649–1678, 2015, doi: 10.1109/COMST.2015.2417576.
- [2] A. Jovicic, J. Li, and T. Richardson, "Visible light communication: Opportunities, challenges and the path to market," *IEEE Commun. Mag.*, vol. 51, no. 12, pp. 26–32, 2013, doi: 10.1109/MCOM.2013.6685754.
- [3] J. Sebastián, P. J. Villegas, F. Nuño, and M. M. Hernando, "High-efficiency and wide-bandwidth performance obtainable from a two-input buck converter," *IEEE Trans. Power Electron.*, vol. 13, no. 4, pp. 706–717, 1998, doi: 10.1109/63.704143.
- [4] D. G. Aller, D. G. Lamar, M. Arias, J. Rodriguez, P. F. Miaja, and J. Sebastian, "Design of a Two Input Buck converter (TIBuck) for a Visible Light Communication LED driver based on splitting the power," *Conf. Proc. - IEEE Appl. Power Electron. Conf. Expo. - APEC*, vol. 2020-March, pp. 1309–1314, 2020, doi: 10.1109/APEC39645.2020.9124254.
- [5] O. García, J. A. Cobos, J. Uceda, and J. Sebastián, "Zero voltage switching in the PWM half bridge topology with complementary control and synchronous rectification," *PESC Rec. - IEEE Annu. Power Electron. Spec. Conf.*, vol. 1, pp. 286–291, 1995, doi: 10.1109/PESC.1995.474825.
- [6] W. Eberle, Y. Han, Y. F. Liu, and S. Ye, "An overall study of the asymmetrical half-bridge with unbalanced transformer turns under current mode control," *Conf. Proc. - IEEE Appl. Power Electron. Conf. Expo. - APEC*, vol. 2, no. C, pp. 1083–1089, 2004, doi: 10.1109/apec.2004.1295957.
- [7] W. Qin, G. Lan, and X. Wu, "A family of ZVSZCS resonant DCX with DC resonant capacitor," *2015 IEEE 2nd Int. Futur. Energy Electron. Conf. IFEEC 2015*, no. c, pp. 6–11, 2015, doi: 10.1109/IFEEC.2015.7361431.
- [8] Y. Ren, M. Xu, C. S. Leu, and F. C. Lee, "A family of high power density bus converters," *PESC Rec. - IEEE Annu. Power Electron. Spec. Conf.*, vol. 1, no. 5, pp. 527–532, 2004, doi: 10.1109/pesc.2004.1355802.
- [9] M. Arias, D. G. Lamar, F. F. Linera, D. Balocco, A. Aguisa Diallo, and J. Sebastián, "Design of a soft-switching asymmetrical half-bridge converter as second stage of an LED driver for street lighting application," *IEEE Trans. Power Electron.*, vol. 27, no. 3, pp. 1608–1621, 2012, doi: 10.1109/TPEL.2011.2164942.